

Defect Generation in p-MOSFETs Under Negative-Bias Stress: An Experimental Perspective

Souvik Mahapatra, *Senior Member, IEEE*, and Muhammad Ashraful Alam, *Fellow, IEEE*

(Invited Paper)

Abstract—In this paper, a focused review is made of our previously reported (2002–2007) work on negative bias temperature instability (NBTI) measurement and analysis. Using suitable cross-reference to other published work, the impacts of stress condition, characterization technique, and gate-oxide process on measured NBTI parameters are reviewed. The large scatter of measured time, bias, and temperature dependencies of NBTI, which are observed in published literature, is carefully analyzed. A common framework for NBTI physical mechanism is suggested and discussed. Issues lacking proper understanding at present are also highlighted.

Index Terms—Bulk traps, charge pumping (CP), hole trapping, hot-hole generation, interface traps, negative bias temperature instability (NBTI), on-the-fly (OTF) I_{DLIN} , p-MOSFETs, reaction-diffusion (RD) model, Si oxynitride.

I. INTRODUCTION

NEGATIVE bias temperature instability (NBTI) of p-MOSFET parameters, i.e., threshold voltage (V_T), linear (I_{DLIN}) and saturation (I_{DSAT}) drain current, transconductance (g_m), etc., is an important reliability concern for modern ICs. Although first observed during 1970s [1], NBTI has resurfaced in the past ten years, both for mainstream digital and analog devices [2]–[9]. This is due to the introduction of surface channel p-MOSFETs for analog circuits and the scaling of gate oxides below 2 nm for digital circuits, without proportionate scaling of supply voltages. In particular, the incorporation of nitrogen in sub-2-nm gate oxides (to prevent boron penetration and reduce gate leakage) has presently made NBTI the most crucial reliability concern [10]–[27].

Like all other reliability phenomena, lifetime estimation for NBT degradation involves accelerated stress (short-duration high stress V_G), which is followed by projection to operating (to end-of-product life, at $V_G = V_{\text{DD}}$) condition. Robust projection requires careful considerations of three issues. First, it is important to choose proper stress condition such that only the damage responsible for NBTI is accelerated and no new

damage mode is triggered [28]–[32]. Second, the measurement techniques must be chosen carefully so that measured data reflect the intrinsic degradation and are not corrupted by any measurement-related artifacts [33]–[36]. Finally, it is also important to understand and model the physical-degradation process [37]–[46] to perform reliable extrapolation from stress to operating condition.

Despite extensive characterization since mid 1990s, there is significant discrepancy regarding the time evolution, temperature (T) activation, and bias dependence of NBTI. Most authors [2]–[21] suggest power-law time dependence ($\sim t^n$) and Arrhenius T activation, although the reported time-exponent ($n \sim 0.08$ – 0.3) and activation-energy ($E_A \sim 0.05$ – 0.2 eV) values show a huge spread. A few other groups have also suggested log-time dependence ($\sim \log t$) [24] and non-Arrhenius T dependence [45], [46]. Similarly, there is a debate if a simple Arrhenius-like T activation is sufficient to capture NBTI temperature degradation or if NBTI is better described by dispersive temperature activation. Finally, some groups suggest that NBTI is a voltage-driven (V_G) phenomenon, while others believe that this degradation is driven by the electric field (E_{OX}) at the Si/oxide interface. Moreover, there is no universally accepted functional form of V_G or E_{OX} dependence of NBTI degradation. Some suggest power-law degradation ($\sim V_G^m$), others prefer an exponential form ($\sim \exp(\beta V_G)$), and still others, a combination of both ($\sim V_G^m \cdot \exp(\beta V_G)$).

A number of attempts have been made to model NBTI [8]–[28], [37]–[46], but given the complexity/diversity of the experimental dataset as discussed earlier, none of the theoretical models have been able to explain NBTI degradation within a common framework. We suggest that this is primarily due to large scatter in published data, as several groups have used different stress conditions, measurement methods, and gate-oxide processes (unspecified chemical composition and thermal treatment). These do not allow unambiguous comparison of experimentally measured parameters and cause significant impediment to develop predictive theory and reproducible analysis and, therefore, have resulted in significant uncertainty regarding the physical mechanism of NBTI—whether it is dominated by interface-trap generation (ΔN_{IT}) or hole trapping (ΔN_h) in preexisting bulk traps and whether bulk oxide traps (ΔN_{OT}) are generated during accelerated NBT stress.

Manuscript received July 17, 2007; revised September 5, 2007.

S. Mahapatra is with the Department of Electrical Engineering, Indian Institute of Technology Bombay, Mumbai 400076, India.

M. A. Alam is with the School of Electrical Engineering and Computer Science, Purdue University, West Lafayette, IN 47907-2035 USA (e-mail: souvik@ee.iitb.ac.in).

Digital Object Identifier 10.1109/TDMR.2007.912261

This paper, which is a focused review of our past work (with suitable reference to other published work), addresses some of the above concerns. It is shown.

- 1) Under proper stress (low stress V_G) when hot-hole generation is negligible, V_T shift is due to the generation of N_{IT} (broken \equiv Si–H bonds at Si–SiO₂ interface) and is controlled by inversion (INV)-layer holes and E_{OX} (not V_G). This is the dominant degradation mode for pure-SiO₂, plasma-nitrided oxide (PNO) having moderate N dose and subjected to proper postnitridation anneal, and thin thermal-nitrided oxide (TNO) with low N dose.
- 2) Additional (to ΔN_{IT}) hole trapping (in preexisting traps) is observed for thicker TNO samples (as also reported in [22]–[24]), which increases the magnitude but reduces n and E_A of overall measured ΔV_T during NBTI stress.
- 3) The above conclusions are based on on-the-fly (OTF) I_{DLIN} measurements (I_{DLIN} degradation is monitored without removing stress [33]) with 1-ms initial (time-zero) delay [35]. Fast OTF experiments with 1- μ s initial delay have been performed on p-MOSFETs having a wide variety of gate insulator process and has been reported elsewhere [21]. It has been reverified that NBTI in PNO MOSFETs (which undergo proper postnitridation anneal and have moderate N dose, such that N density at Si–SiON interface is low) is dominated by N_{IT} generation. It has also been shown that thicker TNO samples (N density at Si–SiON interface is very high) suffer from large ΔN_h (in addition to ΔN_{IT}), which is consistent with conclusions made in this paper and in our recent work [19]. For completeness, it is suggested that this paper be read together with [21] for a review of latest results.
- 4) For conventional stress–measure–stress (SMS) scheme, NBTI recovery during stress-off (measurement) period affects measured n and E_A [33], [34]. Recovery, and hence measured parameters, strongly depends on measurement methodology: I_{DLIN} or charge pumping (CP), sense V_G , delay time, etc., as well as gate insulator process: thickness, N dose, etc. (as also shown in [14]) [20]. OTF I_{DLIN} measurement does not suffer from recovery artifacts and, hence, yield identical NBTI parameters for a wide range of gate insulator-processing conditions.
- 5) The T activation is shown to be Arrhenius, while the signature of non-Arrhenius T activation for SMS measurements, i.e., n linearly dependent on T [45], [46] is shown to be an artifact of measurement delay [15].
- 6) Different measurement techniques (e.g., I_{DLIN} and CP) suffers from different delay and scans different zone in the energy-band gap. Moreover, degradation calculated from OTF I_{DLIN} in its simplest form [14], [15], [33] ignores mobility degradation (details about mobility-correction procedure has been presented elsewhere [36]), which results in inaccurate ΔV_T . Such issues must be accounted for before 1 : 1 comparison can be made across different measurement techniques.
- 7) The magnitude of V_G during NBT stress controls generation of N_{OT} (broken \equiv Si–O bonds, due to impact ionization and hot-hole generation in n -well), which may affect overall ΔV_T and measured n at longer stress time.

TABLE I
PROCESS CONDITIONS OF DEVICES USED IN SECTION II-A.
PNO: PLASMA-NITRIDED OXIDE, TNO: THERMAL-NITRIDED OXIDE. THIN EOT SiO₂ IS USED AS CONTROL OXIDE

D#	Type	EOT (nm)	N% (atomic)	T _{XPS} (nm)	T _{INV} (@V _{FB} -2V) (nm)
P1	PNO	1.23	14	1.51	2.19
P2	PNO	1.23	21	1.67	2.19
P3	PNO	1.64	28	2.27	2.71
P4	PNO	2.14	29	2.85	3.35
T1	TNO	1.19	11	1.25	2.14
T2	TNO	1.15	17	1.44	2.09
T3	TNO	1.85	5	2.1	2.93
T4	TNO	2.2	5	2.3	3.43
C1	SiO ₂	1.36	-	-	2.36

Broken \equiv Si–O bonds show up as stress induced leakage current (SILC) (midoxide defects) [47]–[52], as well as enhanced ΔN_{IT} (near-interface defects) when measured using CP [53]. Stress V_G must be carefully chosen to avoid ΔN_{OT} contribution.

- 8) Time evolution of N_{IT} generation (due to broken \equiv Si–H bonds) during NBT stress can be explained by the reaction–diffusion (RD) approach [37]–[39], [41]–[43], with few discrepancies that are highlighted. The E_{OX} dependence of N_{IT} generation has been explained using hole-assisted field-enhanced model for Si–H bond dissociation. While RD formulation can account for NBTI in most cases as in 1), it needs to be supplemented by hole-trapping model for situations as in 2), which is beyond the scope of this paper and have been discussed in detail elsewhere [35].

II. RESULTS AND DISCUSSION

A. Material Dependence of NBTI Physical Mechanism

The very first step in removing the ambiguity of the published literature is to realize that various components of NBTI degradation (i.e., N_{IT} , N_{OT} , N_h) depend on oxide composition and process conditions. To verify this, devices having different process conditions are used in this paper to explore the material dependence of NBTI, as shown in Table I, fabrication details of which can be found in [54]. Films with various thicknesses and N dose have been studied for both PNO and TNO. For a given N dose, peak N density is located at the Si–SiON interface for TNO and at the SiON–poly-Si interface for PNO [55], [56]. PNO films were subjected to proper postnitridation anneal to improve the film quality. Thin SiO₂ was used as a control oxide. The equivalent oxide thickness (EOT) of these films were obtained from C – V measurements and analyzed subsequently with a well-calibrated C – V model with appropriate quantum–mechanical corrections.

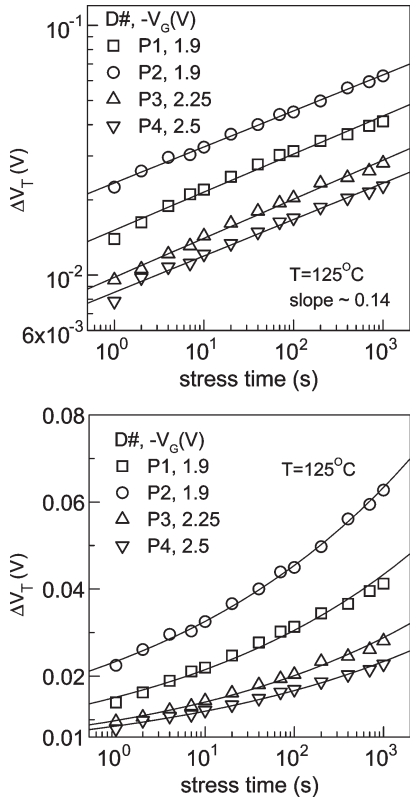


Fig. 1. Time evolution of ΔV_T obtained from OTF I_{DLIN} measurements for PNO devices, which is plotted in a (top) log–log and (bottom) semilog scale.

V_T shift during NBT stress is extracted using OTF I_{DLIN} [33] with 1-ms initial delay, using the expression $\Delta V_T = -\Delta I_D / I_{D0} (V_G - V_{T0})$ [14], [15], where I_{D0} is the initial I_{DLIN} measured within 1 ms of the application of stress, V_G is stress bias, and V_{T0} is the prestress V_T . The obtained ΔV_T is slightly different than the actual, as mobility degradation is not taken into account (as discussed in [36]). CP measurement was done on separately stressed samples for direct determination of interface traps when required, after interrupting stress at log time intervals (SMS). Single-frequency fixed-amplitude gate pulse is used during such CP measurement to minimize stress-interruption time. The top and base level of the CP gate pulse was chosen sufficiently higher than flatband and lower than threshold-voltage levels, respectively. This ensures that any charge-trapping-induced shift in these levels does not significantly alter the CP area after stress [53].

Fig. 1 shows the time evolution of ΔV_T for different PNO films plotted in a log–log (top) and semilog (bottom) scale. It can be clearly observed that ΔV_T shows power-law (t^n) and not log time dependence, with asymptotic slope of $n \sim 0.14$ for all PNO splits. Fig. 2 shows the time evolution of ΔV_T for thin and thick TNO films plotted in a log–log scale (top) and for thick TNO films plotted in a semilog scale. Thin TNO film shows identical power-law time evolution of ΔV_T , as in PNO, and does not show log time dependence when plotted in a semilog scale (not shown). On the other hand, thick TNO device shows very high NBTI degradation and lower n (~ 0.09) when plotted in a log–log scale and almost perfect log time dependence when plotted on a semilog scale.

Fig. 3 shows the stress V_G and T dependence of power-law time exponent for PNO (all splits) and thin TNO devices. The

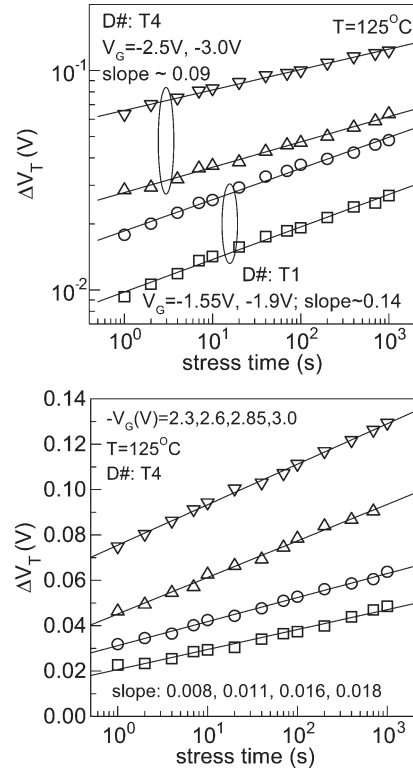


Fig. 2. Time evolution of ΔV_T obtained from OTF I_{DLIN} measurements at different stress V_G for (top) thin and thick TNO devices plotted in a log–log scale, and (bottom) thick TNO device plotted in a semilog scale.

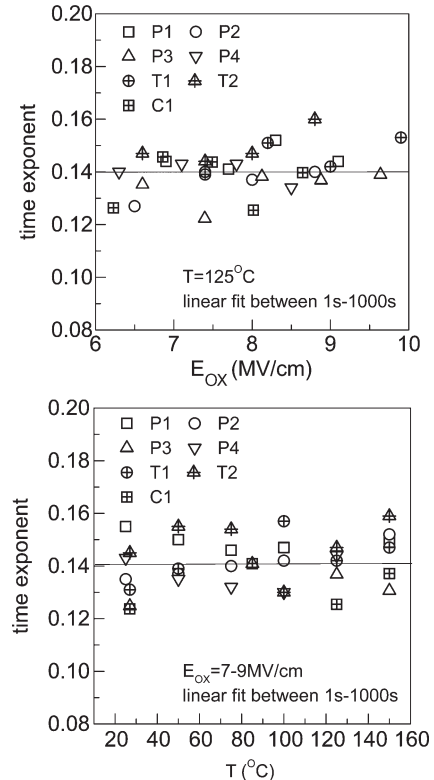


Fig. 3. Extracted power-law time exponent from OTF I_{DLIN} measurements for PNO and thin TNO devices for different (top) stress V_G and (bottom) stress T .

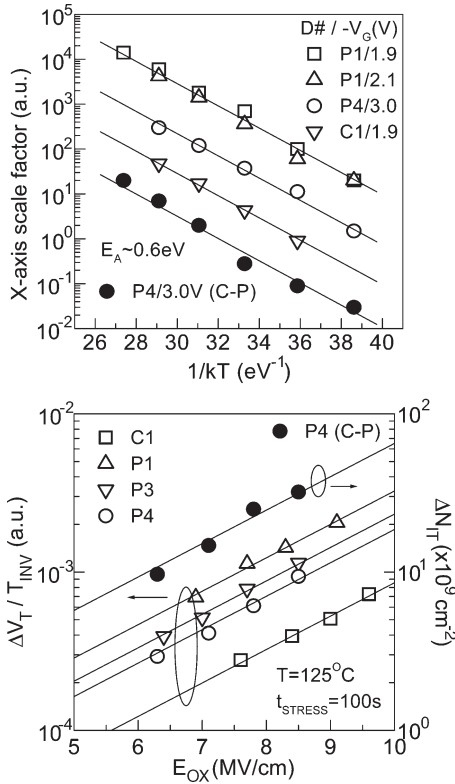


Fig. 4. (Top) T activation extracted at constant degradation and (bottom) E_{OX} dependence extracted at constant time, for different PNO devices from OTF I_{DLIN} measurements and for thick PNO devices from CP measurements.

scatter in n is due to noise during I_{D0} measurement. Note that the mean value of n is approximately 0.14 and is consistent across all the devices used in this paper. The T and V_G independence of n has important implications (as discussed later) and asserts the universality of underlying physical mechanism. Note that, similar to the impact of delay during SMS measurement [33], [34], time-zero delay also affects measured n , as shown in [27]. It is, therefore, possible that the n obtained with such relatively “slower” OTF is not accurate, and all devices would show somewhat lower n when measured with “faster” OTF. Indeed, fast OTF (with initial delay of $t_0 = 1 \mu s$) measurements in similar PNO samples show that $n \sim 0.12$, although the variation on n with t_0 has been found to be insignificant (within error) for t_0 in the range of 1–100 μs (as reported elsewhere [21]). Fast OTF measurements in thick TNO samples show that $n \sim 0.06$, which is much lower than that for PNO because of dominance of hole trapping [23]. Finally, PNO samples fabricated without postnitridation anneal show very high NBTI degradation and lower n (~ 0.08) when measured using fast OTF, which is similar to thick TNO samples (not shown). To summarize, the time exponent of NBTI degradation—a topic of much debate and disagreement in the literature—is a reflection of variously processed oxides used by different groups, and for similarly processed devices, the time evolution is unambiguous and universal.

The material-dependent E_{OX} and T characteristics of NBTI degradation are considered next. Fig. 4 (top) shows the T activation of NBTI obtained at a fixed level of degradation by time-axis scaling of T -dependent $\Delta V_T(t)$ data for various PNO

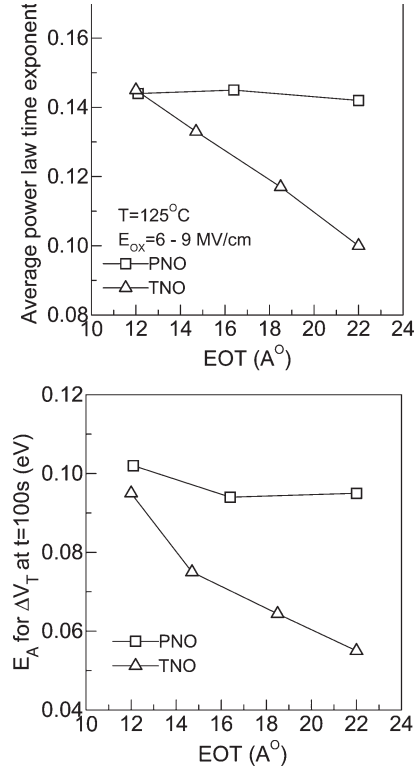


Fig. 5. EOT dependence of (top) average power-law slope and (bottom) T activation at fixed time for PNO and TNO devices.

(varying N dose and EOT) and control samples. The activation energy so obtained is defined as activation of diffusion, $E_A(D)$, for reasons explained in Section II-D [8]. Identical $E_A(D)$ is obtained for all splits, which also equals to that obtained from similar time-axis scaling of T -dependent $\Delta N_{IT}(t)$ data (from CP) for thick PNO samples [17], [20]. Fig. 4 (bottom) shows the E_{OX} dependence of ΔV_T (normalized to INV oxide thickness T_{INV}) for control as well as thin (lower N dose) and thick (higher N dose) PNO films. The E_{OX} dependence of ΔN_{IT} (obtained on thick PNO films using CP) is also shown. For a given E_{OX} , ΔV_T magnitude is higher for PNO as compared to SiO_2 as expected, while it decreases with increase in EOT for PNO films (in spite of higher N dose for thicker films). However, identical E_{OX} -dependent slopes are obtained for SiO_2 and PNO films, which equal to the slope of E_{OX} dependence of ΔN_{IT} (from CP).

Fig. 5 (top) shows the average power-law time exponent (obtained from log–log plot), and Fig. 5 (bottom) shows E_A (obtained at fixed time from T -dependent data) as a function of EOT, from OTF I_{DLIN} measurement on PNO and TNO devices [18]. Averaging in n takes care of experimental scatter, as shown in Fig. 3. Note that E_A obtained at fixed stress time is different from $E_A(D)$ and is discussed in Section II-D. For PNO, the obtained n and E_A are independent of EOT in the range studied. However, for the TNO device, both n and E_A increase with reduction in EOT, and the smallest EOT TNO shows similar n and E_A as PNO devices.

It is generally believed that N_{IT} generation would show power-law time dependence and strong T activation [8], [14], [15], [17], [19], while hole trapping in preexisting traps would show log time dependence and weak T activation [23]–[27].

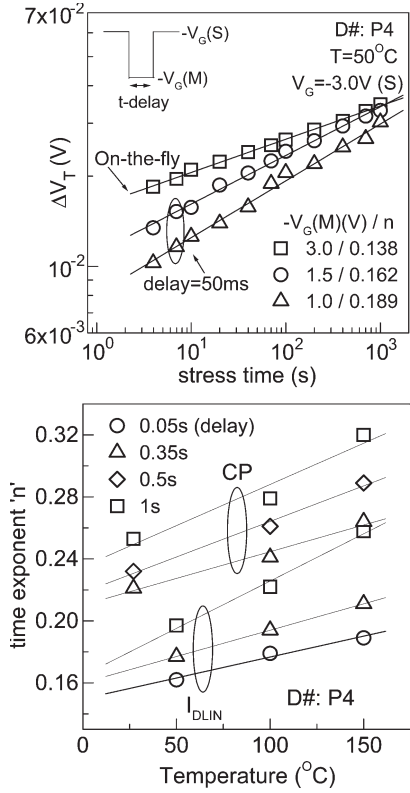


Fig. 6. (Top) Time evolution of ΔV_T obtained from OTF I_{DLIN} ($V_{G,STRESS} = V_{G,MEAS}$) and delay I_{DLIN} ($|V_{G,STRESS}| > |V_{G,MEAS}|$, as shown in inset) techniques and (bottom) time exponent of degradation for various stress T and measurement delay time, obtained from delay I_{DLIN} and CP measurements.

Note that power-law time dependence (Fig. 1), very similar n for a wide range of stress V_G and T (Fig. 3), strong T activation, and identical $E_A(D)$ and E_{OX} dependencies for I_{DLIN} and CP measurements (Fig. 4), suggests that NBTI in PNO films is dominated by the generation of N_{IT} . This is also consistent with EOT independence of n and E_A for such films (Fig. 5). The very high NBTI degradation (Fig. 2) with log time dependence (or power-law dependence with low n) and low T activation (Fig. 5) suggest ΔN_h -driven NBTI for thick TNO. As EOT is reduced, hole-trapping volume reduces, and therefore, n and E_A increases for TNO films. Thin TNO shows identical n and E_A as PNO, and NBTI in such films is again dominated by N_{IT} generation [17], [19]. Modeling of N_{IT} generation is discussed in Section II-D.

B. Measurement (Method, Delay)-Related Issues

As discussed in the Introduction, measurement-artifact-free NBTI data are a prerequisite for robust theoretical analysis of NBTI degradation. It is now well known that NBT-stress-induced degradation recovers significantly after the stress is removed [14], [25]–[27], [33], [34]. Therefore, conventional SMS schemes show recovery-induced artifacts, such as lower degradation magnitude and higher n [33], [34]. Fig. 6 (top) shows time evolution of ΔV_T that is obtained from the following: 1) OTF I_{DLIN} [33] and 2) delay I_{DLIN} (gate bias moves down from stress to measurement voltage, I_{DLIN} is measured, and then gate bias moves back to stress [45]) at varying-

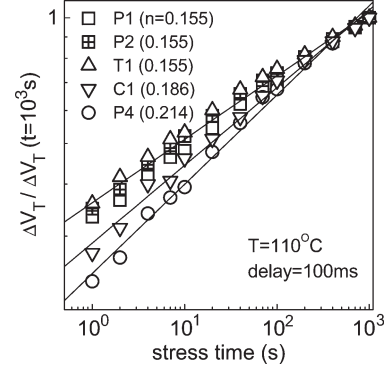


Fig. 7. Time evolution of ΔV_T for various splits (as shown in Table I) obtained from delay I_{DLIN} measurements.

measurement gate voltage ($V_{G,MEAS}$). Note that, for delay I_{DLIN} measurement, not only the measurement-related (stress-off) delay time (t -delay) but also $V_{G,MEAS}$ strongly influences the slope and magnitude of ΔV_T . Lower magnitude and higher n are measured, as t -delay is increased [33], [34] or for a given t -delay as $|V_{G,MEAS}|$ is lowered [15]. While the impact of t -delay on measured n is relatively easy to comprehend, the impact of $|V_{G,MEAS}|$ (or, for that matter, whether the gate has transitioned directly from stress to measurement or transitioned via 0 V) is more subtle, not always well appreciated, yet it equally affects NBTI measurement. Fig. 6 (bottom) shows the measured power-law time exponents from delay I_{DLIN} and CP measurements for various T and t -delay [20]. For a given t -delay, n increases with increase in T and may suggest non-Arrhenius T activation [45], [46]. However, the phenomenon is a recovery artifact as it reduces with a reduction in t -delay and n becomes independent of T for OTF, as described in the previous section. Furthermore, it is important to note that, for a given T and t -delay, n (and hence, recovery) is higher for CP than I_{DLIN} [20]. This is expected, since unlike I_{DLIN} , V_G become positive during CP measurements, leading to higher recovery. Difference in recovery between I_{DLIN} and CP measurements creates complications for direct comparison (as done in [23]) and is discussed later.

Fig. 7 shows the time evolution of ΔV_T for various gate-insulator processes (variation in thickness and nitrogen dose, see Table I) obtained from delay I_{DLIN} measurements [20]. Since OTF measurements show identical n for all these splits, the difference in n between different splits is due to the difference in recovery. It is observed that thin PNO and TNO samples show very similar n (and, hence, recovery), irrespective of N dose (within 10%–20% range as studied in this paper), which is lower than that for SiO_2 films having similar EOT. For thicker PNO films, n increases with increasing EOT and implies increased recovery with increasing film thickness. Similar material dependence of recovery has recently been reported [14]. It is evident that delay I_{DLIN} or similar conventional SMS measurements would introduce significant uncertainty in measured degradation and cannot be used for reliable estimation of NBTI degradation.

Note that identical T activation and E_{OX} dependence of I_{DLIN} and CP results for thick PNO (as shown in Fig. 4) suggests N_{IT} -generation-driven V_T shift for such films. This

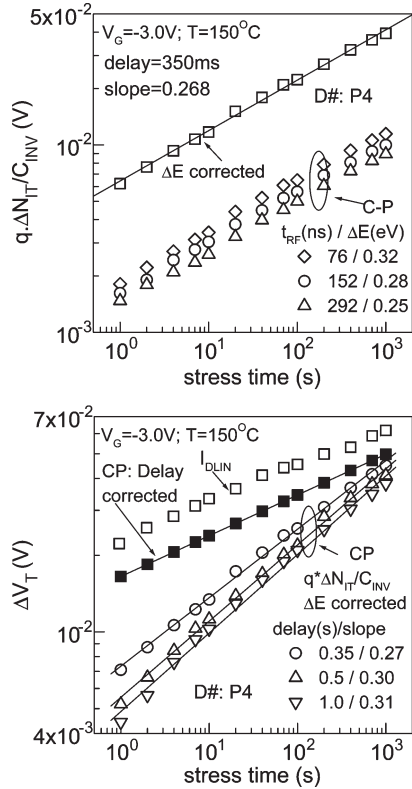


Fig. 8. Time evolution of ΔV_T from CP (top) for various rise/fall time of gate pulse and corrected for difference in ΔE with respect to I_{DLIN} , and (bottom) time evolution of ΔV_T from OTF I_{DLIN} and from CP for various measurement delay, but corrected for ΔE . Additional correction for delay is done on CP data using RD model solution, to compare with I_{DLIN} data.

is because, while I_{DLIN} measures total ΔV_T due to ΔN_h and ΔN_{IT} , CP measures the contribution that is due to ΔN_{IT} only. Therefore, a simple and direct comparison of NBTI magnitude from I_{DLIN} and CP would ideally be a much straightforward method to estimate whether ΔV_T can be entirely attributed to ΔN_{IT} alone or not. Indeed, the difference of absolute levels of NBTI degradation, as measured by CP and I_{DLIN} methods, has been used to isolate relative contributions from N_{IT} and N_h and to suggest that hole trapping (N_h) dominates NBTI degradation, presumably in all films [23]. However, such straightforward analysis is not possible due to the following reasons [19]. First, inherent delay and large recovery associated with CP would cause lower ΔV_T magnitude during NBTI stress. Moreover, the energy zone in the band gap scanned by CP (near midgap [53]) is quite different from that scanned by I_{DLIN} (full band gap E_G). Therefore, the generation of ΔV_T , as directly measured from CP and I_{DLIN} , cannot be compared to each other, as in [23], without correcting for differences in scanned energy zones in the band gap and measurement delays. A first-order correction procedure is discussed as follows.

Fig. 8 (top) shows the time evolution of ΔV_T for thick PNO device obtained from CP measurements with different rise and fall times of the gate pulse. Energy zone in the band gap (ΔE) scanned by CP increases with the reduction in rise–fall time, resulting in higher ΔI_{CP} and calculated $\Delta V_T (= q \cdot \Delta N_{IT} / C_{INV})$, C_{INV} is the gate capacitance in INV) magnitude (see [53] for details). Note that the extracted CP energy zones are much smaller than E_G . Hence, the difference in CP

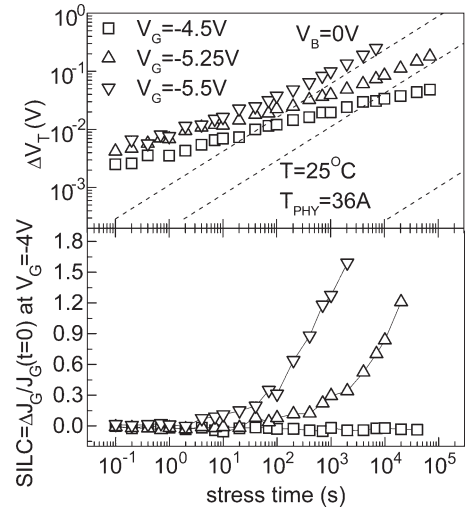


Fig. 9. Time evolution of (top) threshold-voltage degradation and (bottom) stress-induced leakage current for various stress-gate bias. Stressing was done on a 36 A° p-MOSFET at 27°C in INV. SILC was measured at $V_G = -4 \text{ V}$.

and I_{DLIN} energy zones must be accounted for by multiplying the CP data with the $E_G/\Delta E$ ratio as a first step toward direct comparison, as shown [19]. Note that (NBT-stress-induced) generation of donorlike N_{IT} throughout the band gap is assumed for this calculation. This model can successfully explain the skew in $C-V$ curve after the NBT stress [57], without assuming any unrealistic 1 : 1 correlation of interface traps and fixed charges. However, any localized (near the edges in energy band gap [58]) peak in trap generation while detected by I_{DLIN} cannot be accounted for when CP data are corrected for the difference in ΔE , as done earlier, and would result in lower ΔV_T estimation.

Fig. 8 (bottom) shows the time evolution of ΔV_T for thick PNO device obtained from CP measurements, after ΔE correction (as described earlier) but with different measurement delay. ΔV_T obtained from OTF I_{DLIN} is also shown. Reduced delay reduces n and increases ΔV_T magnitude. Therefore, zero-delay data must be calculated as a second step for direct comparison of CP and I_{DLIN} results. When corrected¹ based on RD model with molecular H_2 diffusion (as justified later in Section II-D), the difference between ΔV_T obtained from I_{DLIN} and CP reduces to within 20% of each other (without accounting for any localized peak interface-trap generation near the CB edge in the band gap) and not $\sim 10 \text{ X}$, as one would obtain (and, therefore, conclude ΔN_{IT} contribution to ΔV_T is negligible [23]) if the differences in measurement delay and energy zones are not taken into account.

C. Stress-Bias-Related Issues

As aforementioned, it is important to choose the correct measurement method for proper estimation of NBT degradation. Similarly, it is also equally important to choose the proper stress condition, such that only NBTI-related defects are accelerated and no new defects are formed. Fig. 9 (top) shows the time

¹Fractional recovery is measured (separately) after 1000-s stress and unrecovered ΔV_T (at $t = 1000 \text{ s}$) is calculated. For $t < 1000 \text{ s}$, $\Delta V_T(t)$ data are generated using specified RD solution trend line ($n \sim 1/6$).

evolution of ΔV_T for thick SiO₂ p-MOSFET under INV stress at different V_G . ΔV_T is obtained from I_D - V_G measurements, after interrupting stress at log time intervals (SMS measurement scheme). At low V_G , ΔV_T shows power-law time dependence (t^n) with $n \sim 0.25$ for the entire stress window (the impact of measurement delay on n is discussed in Section II-B). At high V_G , ΔV_T shows identical (as low V_G) degradation rate for short stress time but breaks off from the initial trend and drastically increases at long stress time. The break-off time decreases and postbreak slope increases as stress V_G is increased [8], [28]. Such behavior has also been observed in thinner oxynitride devices [30] and needs careful attention.

To check whether such atypical features in ΔV_T is due to bulk-trap contribution, Fig. 9 (bottom) plots SILC ($\Delta J_G(t)/J_G(t=0)$, plotted in a semilog scale) under identical stress conditions. SILC was also measured by interrupting stress at log time intervals (on separate samples), and multiple I_G - V_G sweeps were performed to nullify any effect due to trapped charges (transient SILC) [47]. SILC uses mid-thickness bulk traps for conduction and, therefore, correlates well with bulk-trap generation [48]. While not seen for low V_G stress, SILC is clearly observed for high V_G stress (and shows the characteristic $t^{1/2}$ time dependence when plotted in a log-log scale, not shown), indicating bulk-trap generation. It is clear from Fig. 9 that the onset and magnitude of SILC matches very well with that for ΔV_T under identical stress conditions. Note that the bulk traps responsible for SILC are generally believed to be neutral [49]. However, since SILC and long-time enhanced ΔV_T shows identical time exponent and voltage acceleration, we believe a fraction of these neutral traps capture holes, become positively charged, and contribute to ΔV_T . This is verified by calculating the contribution of ΔN_{OT} to overall ΔV_T , as shown using dashed lines in Fig. 9 (top) [8], [28]. Indeed, the asymptotic ΔV_T at high-stress V_G shows voltage acceleration of 4.95 V/dec, which is identical to that obtained for ΔN_{OT} [50]. Therefore, we conclude that there could always be a significant ΔN_{OT} contribution to NBTI data if stress V_G is too high.

Having established the generation of bulk traps during NBT stress, it is important to understand the physical origin of this process so that one could stay in safe test regions (avoid ΔN_{OT} contribution) for all oxide thickness and voltage conditions. To explain the role of stress bias, Fig. 10 (top) shows the energy-band diagrams for p-MOSFET under constant voltage stress in INV as follows: 1) low V_G ($V_B = 0$); 2) high V_G ($V_B = 0$); and 3) low V_G but high V_B . At all (low to high) V_G , N_{IT} generation due to breaking of $\equiv \text{Si}-\text{H}$ bonds at Si-SiO₂ interface (as shown in Fig. 10 bottom) is triggered by either electrons that tunnel from poly-Si to substrate or by holes that are present at the substrate and tunnel into the oxide, as shown in Fig. 10(a) (more on this in Section II-D). At high V_G ($V_B = 0$), N_{OT} generation (breaking of $\equiv \text{Si}-\text{O}$ bonds at oxide bulk, see Fig. 10 bottom) is triggered by impact ionization and hot-hole generation at the substrate, as shown in Fig. 10(b) (top) [50], [51]. This is consistent with the fact that a high-stress V_B at low V_G keeps E_{OX} low but independently increases the hot-hole population [see Fig. 10(c) (top)] and results in similar enhancement of degradation (see as follows and also [8], [28], [31]).

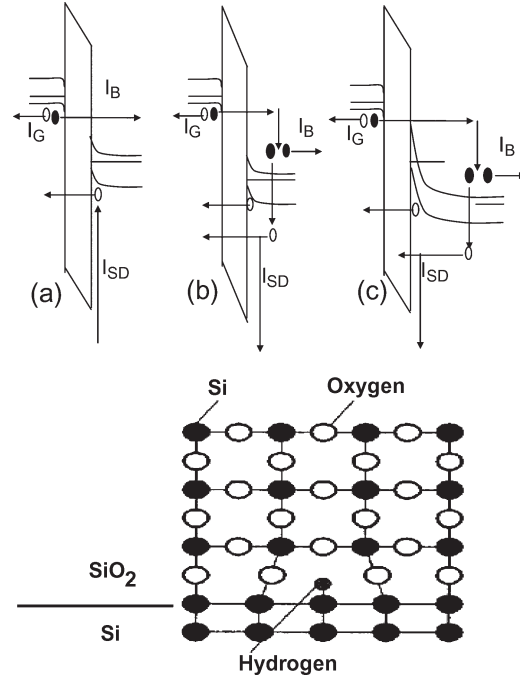


Fig. 10. Energy-band diagrams for p-MOSFET (p+ poly-Si, n-type substrate) under constant voltage stress in INV for (a) low gate bias, (b) high gate bias, and (c) high substrate bias at low gate bias, electron (solid circles) and hole (open circles) currents are shown (top), and schematic of Si-SiO₂ system showing $\equiv \text{Si}-\text{O}$ and $\equiv \text{Si}-\text{H}$ bonds (bottom).

As shown in Fig. 10 (top), hot-hole generation is governed by gate leakage and quantum yield (QY) (efficiency of an electron tunneling into the substrate from gate to create impact ionization [52]). While the gate leakage is governed by gate-insulator thickness and N concentration, QY is related to the energy of electrons and, hence, stress V_G . To achieve a particular E_{OX} during NBTI stress, thicker insulators would require higher V_G but would show lower gate leakage, and thinner insulators would require lower V_G but would show higher gate leakage. Therefore, it is difficult to define a general upper limit of “safe” E_{OX} (or V_G) during NBT stress. However, for sub-2-nm films (which are of particular interest at present), experiments (n independent of stress V_G) have shown that up to about E_{OX} of 9 MV/cm can be considered as safe to avoid generation of bulk traps.

As discussed above, broken $\equiv \text{Si}-\text{O}$ bonds (in the presence of hot holes) at the oxide bulk shows up as SILC. It is therefore possible that broken $\equiv \text{Si}-\text{O}$ bonds near the Si-SiO₂ interface would be detected by CP measurements [53] and show up as additional interface traps. Fig. 11 shows the time evolution of ΔN_{IT} (measured by CP) in SiO₂ p-MOSFET stressed under different V_B but constant V_G [31]. Increasing V_B stress was used to generate increasing amount of hot holes in the channel by impact ionization [see Fig. 10(c) top]. ΔN_{IT} shows the usual power-law time dependence, with relatively² lower n for stress at $V_B = 0$. ΔN_{IT} increases with hot-hole energy as stress V_B is increased, and the power-law signature is maintained although with a higher value of n . Note that the break-time (time

²The absolute value of n is large due to recovery artifacts, see Section II-B.

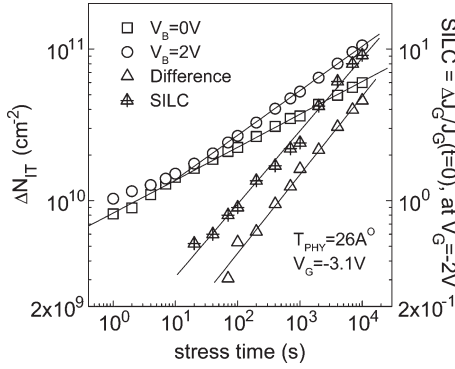


Fig. 11. Time evolution of interface-trap density for $V_B = 0$ and 2-V stress. Stressing was done on 26 Å p-MOSFETs at $T = 27$ °C in INV. Time evolution of $V_B = 2$ V stress-induced enhanced-interface trap density and SILC are also shown. SILC was measured at $V_G = -2.0$ V.

beyond which $V_B > 0$ induced ΔN_{IT} enhancement shows up) reduces as V_B is increased (not shown). Time evolution of $V_B > 0$ stress-induced additional degradation $\{\Delta^2 N_{IT} = \Delta N_{IT}(V_B > 0) - \Delta N_{IT}(V_B = 0)\}$, together with measured high- V_G SILC are also shown in Fig. 11. Additional ΔN_{IT} and SILC were observed only for $V_B > 0$ stress under significant hot-hole generation (this is similar to that discussed before), both show good correlation with QY [52] of hot-hole generation as V_B is increased [29] and show power-law time dependence with very similar power-law slope ($n \sim 0.5$) characteristics of bulk-trap generation [50].

Therefore, measured N_{IT} generation has two different origins due to broken \equiv Si-H and \equiv Si-O bonds (Fig. 10 bottom) [32]. When hot-hole generation is insignificant, N_{IT} is due to broken \equiv Si-H bonds at the Si-SiO₂ interface and subsequent diffusion of released hydrogen (discussed in detail in Section II-D). Additional \equiv Si-H bonds can get broken in the presence of hot holes. However, since hot-hole density is much less than that of INV-layer (cold) holes, hot-hole-induced broken \equiv Si-H bonds would be insignificant as compared to \equiv Si-H bonds broken by cold INV-layer holes. In the presence of large hot-hole generation (when the magnitude of stress V_G or V_B is high), broken \equiv Si-O bonds at or very close to the Si-SiO₂ interface makes additional contribution and increases the overall magnitude and n of measured ΔN_{IT} . As discussed earlier, care should be taken to avoid breaking \equiv Si-O bonds during NBT stress. In the next section, a possible mechanism of breaking \equiv Si-H bonds is discussed.

D. Interface-Trap-Generation Mechanism

Having established that the presence of hot-holes during NBT stress breaks \equiv Si-O bonds, which must be avoided during accelerated stress, it is important to identify how \equiv Si-H bonds get broken so that proper voltage-acceleration models can be developed. Here, we consider films that have negligible hole-trapping. Fig. 12 (left-hand side) plots stress V_G and E_{OX} required to achieve a particular $\Delta N_{IT} (= C_{OX}/q \cdot \Delta V_T)$, C_{OX} being oxide capacitance) at a particular stress time, for SiO₂ p-MOSFETs having different oxide thickness (T_{PHY}) [8], [9]. Excellent correlation is observed across physical thickness (T_{PHY}) when ΔN_{IT} is correlated to E_{OX} and not V_G (similar

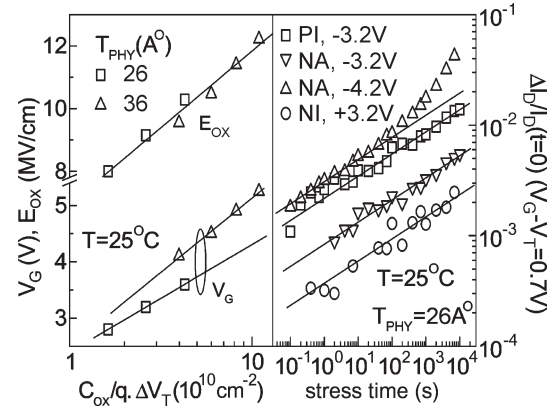


Fig. 12. Stress V_G and E_{OX} required to obtain a particular degradation for p-MOSFETs having different T_{OX} (left-hand side) and time evolution of normalized linear drain-current degradation measured at a fixed-gate overdrive for p- and n-MOSFETs stressed at RT in INV and ACC (right-hand side).

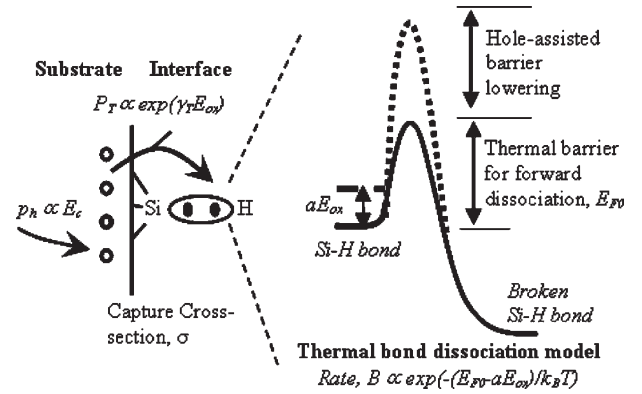


Fig. 13. Schematic representation of a hole-assisted field-enhanced thermal dissociation of interfacial \equiv Si-H bonds.

conclusion was also obtained in [12]), which suggests N_{IT} generation due to broken \equiv Si-H bonds is an E_{OX} - (not V_G , as suggested in [39])-driven phenomenon. Fig. 12 (right-hand side) plots $\Delta I_D(t)/I_D(t=0)$ for SiO₂ p- and n-MOSFETs (identical T_{PHY}) stressed in INV and accumulation (ACC). I_D was measured at a fixed gate overdrive ($V_G - V_T$), which nullifies any trapped-charge effect and reflects mobility degradation. Note that due to V_{FB} differences, $V_{G,ACC} = V_{G,INV} \pm 1$ V for identical E_{OX} during ACC and INV stress [8]. It is shown that ΔN_{IT} depends on the following: 1) E_{OX} , i.e., p-MOSFET stressed in INV and n-MOSFET stressed in ACC show similar ΔI_D at identical E_{OX} and not at identical V_G and 2) hole density (P), i.e., for identical E_{OX} , ΔI_D is largest for p-MOSFET stressed in INV and n-MOSFET stressed in ACC (holes at Si/SiO₂ interface), followed by p-MOSFET stressed in ACC (holes tunnel from p⁺ poly gate) and n-MOSFET stressed in INV (holes generate and tunnel from n⁺ poly gate). It is evident from the earlier discussion that both INV hole density and E_{OX} (not electron gate current and V_G [39]) are responsible for the generation of N_{IT} during NBT stress.

A hole-assisted field-enhanced thermally activated \equiv Si-H bond-breaking (generation of N_{IT}) mechanism is shown in Fig. 13 (see [18] for detailed modeling). Under a favorable E_{OX} , INV layer holes (density proportional to E_C , which is

a semiconductor field to support INV layer) tunnels through the valence-band barrier at the Si–SiO₂ interface (probability $\sim \exp(\gamma_T \cdot E_{OX})$) to \equiv Si–H bonds and get captured. The original energy barrier for the breaking of \equiv Si–H bonds get reduced from E_F to $E_{F0} - \alpha \cdot E_{OX}$ (E_F to E_{F0} due to hole capture and by an additional amount $\alpha \cdot E_{OX}$ due to field-induced dipole stretch-out, where α is the \equiv Si–H dipole-polarization factor). The weak \equiv Si–H bonds subsequently get broken by thermal excitation (rate $\sim \exp(-(E_{F0} - \alpha \cdot E_{OX})/kT)$). The released H diffuses out and determines the time evolution of N_{IT} generation [37]–[39], [41]–[43], [45], [46].

According to the existing RD approaches, the nature of diffusing H species and the type of diffusion determines the power-law time-exponent n . Classical Arrhenius-activated (n independent of stress T) diffusion models suggest $n = 0.16$ for H₂, $n = 0.25$ for H⁰, and $n = 0.5$ for H⁺ diffusion [42], [59]. Dispersive-diffusion models (n linearly dependent on stress T) suggest $n \leq 0.16$ for H₂, $n \leq 0.25$ for H⁰ and $n \leq 0.5$ for H⁺ diffusion [45], [46]. As measured n is independent of T for OTF measurements (within experimental scatter, see Fig. 3), it rules out any substantial dispersive diffusion of hydrogen (note that T dependence of n is an artifact of measurement delay [15]). The classical diffusion model correctly suggests T independence of n , although it predicts somewhat higher n (~ 0.16) than measured ($n \sim 0.14$ for standard OTF, which slightly reduces and saturates to $n \sim 0.12$ for fast OTF [21] in PNO samples, where NBTI is presumed to be dominated by N_{IT} generation). This small difference in time exponents can be due to one or more of the following reasons: 1) measurement issues (small overshoot in I_{D0} during OTF), 2) small dispersion in diffusion of H₂ in poly-Si [43], 3) possible reflection at the poly-Si/oxide interface due to differences in H₂ diffusion coefficients [59], and 4) N_{IT} screening related reduction of E_{OX} at the Si–SiO₂ interface at high-stress time [35]. A detailed discussion on these nonideal effects is beyond the scope of this paper, but as such, we proceed to explain the broad features of N_{IT} generation during NBT stress by classical idealized RD approach. In addition, note that any additional hole-trapping (in thicker TNO samples or not properly optimized PNO samples) must be separately treated, which has been discussed elsewhere [35] and will not be discussed here.

The solution of classical RD model suggests [8], [43], [59]

$$\begin{aligned} C_{INV}/q^* \Delta V_T &= \Delta N_{IT} \\ &= [k_F \cdot N_0/k_R]^{2/3} \\ &\quad * [D_0 \exp(-E_A(D)/kT)t]^n \end{aligned} \quad (1)$$

where n is the power-law time exponent, k_F and k_R are the forward- and reverse-reaction rates (breaking and annealing of \equiv Si–H bonds), N_0 is the total density of \equiv Si–H bonds before stress, D_0 and $E_A(D)$, respectively, are the prefactor (T independent) and activation energy of diffusion for molecular H₂. It is expected that k_F and k_R are similar in magnitude, as ΔN_{IT} stress and recovery are readily observed even at RT [31]. Assuming that $k_F \sim k_R$ in (1), $\Delta V_T(t)$ data obtained at different T can be scaled in time (at constant ΔV_T) to obtain activation of diffusion $E_A(D)$. Note that the magnitude of $E_A(D)$

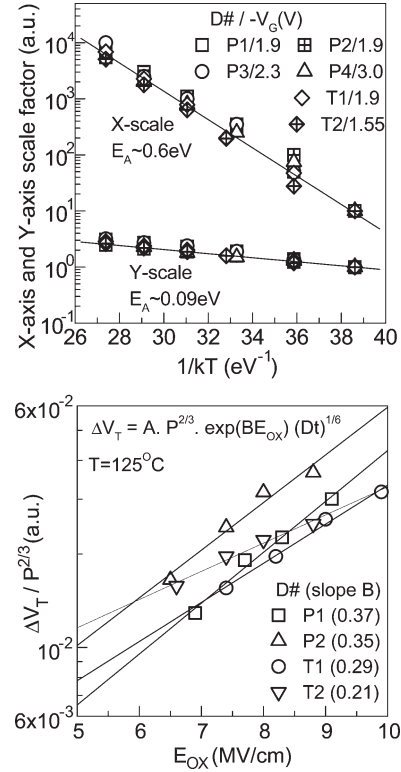


Fig. 14. Constant time scaling (along Y-axis) and constant degradation-level scaling (along X-axis) factors obtained from T -dependent $\Delta V_T(t)$ data (top) and E_{OX} dependence of ΔV_T plotted according to the relation $\Delta V_T = A \cdot P^{2/3} \exp(B \cdot E_{OX})$ (bottom), which is obtained from OTF measurements for different splits.

[identical for I_{DLIN} and CP measurements, as shown in Fig. 4 (top)] suggests molecular H₂ diffusion [60], which is consistent with the obtained value of n . Furthermore, note that the overall activation of degradation (at constant time) is governed by the activation of diffusion by the relation $E_A(\Delta V_T) = E_A(D)^*n$ [8], [43].

Fig. 14 (top) shows the constant time (Y-axis) and constant ΔV_T (X-axis) scale factors obtained using T -dependent $\Delta V_T(t)$ data for PNO, thin TNO, and control samples [8], [9]. The activation energy for overall NBTI, $E_A(\Delta V_T)$, is related to $E_A(D)$ by the exponent n as expected from the RD model solution. The scaling scheme holds for a wide range of splits, again confirming the universality of the underlying physical mechanism. It is important to note that as $E_A(D)$ is the physical quantity, measured E_A of overall NBTI (at fixed time) is dependent on measurement delay, hence n . This has important implication during E_A determination of overall NBTI by conventional SMS methods, as well as comparing E_A obtained by different techniques (e.g., E_A from CP will never be the same as that from I_{DLIN}). Fig. 14 (top) unequivocally shows that N incorporation (for PNO and thin TNO, in the range of dose and EOT studied) does not change the underlying physical mechanism of NBTI, i.e., N_{IT} -generation-driven V_T shift during stress.

As the diffusion species is neutral, E_{OX} dependence of NBTI is governed by the term $[k_F \cdot N_0/k_R]^{2/3}$ [see (1)], which refers to detailed balance between breaking and annealing (of \equiv Si–H bonds) terms. As the reaction term is believed to be

caused by tunneling of INV layer holes into interfacial \equiv Si–H bonds (as described before, see Fig. 13), $[k_F \cdot N_0/k_R]^{2/3} \sim P^{2/3} \exp(B \cdot E_{OX})$, where P is the INV hole density, and (1) can be rewritten as [20]

$$\Delta V_T = A \cdot P^{2/3} \exp(B \cdot E_{OX})^* [D_0 \exp(-E_A(D)/kT)t]^n \quad (2)$$

where A , B , and D_0 can be functions of N concentration. Fig. 14 (bottom) shows the E_{OX} dependence of ΔV_T plotted according to (2) for various thin PNO and TNO films [20]. The field acceleration factor B reduces negligibly with increasing N content for PNO films (control film shows $B = 0.38$, not plotted). However, for TNO films, B reduces drastically with increasing N dose. For a given dose, B is much higher for PNO compared to TNO films. As NBTI is due to INV layer holes tunneling into (and assist in breaking) interfacial \equiv Si–H bonds, N near the Si–SiO₂ interface would lower the tunneling barrier (and also possibly reduce the reaction energy [11]) and hence cause higher N_{IT} generation and hence higher NBTI. For a given total nitrogen dose, TNO films have higher N concentration at the Si–SiO₂ interface as compared to PNO films [55], [56], which explains the larger reduction in B for TNO as compared to PNO films. Moreover, this also explains why ΔV_T (normalized to T_{INV}) for PNO films reduces at higher EOT in spite of higher total N dose for thicker films. Lower B for TNO films implies higher NBTI as E_{OX} is scaled down from the stress to operating conditions. Therefore, reduction in NBTI lifetime with increasing N dose would be more for TNO when compared to PNO.

III. CONCLUSION

To summarize, interface-trap generation (ΔN_{IT}), hole trapping in preexisting traps (ΔN_h), and bulk-trap generation with subsequent hole trapping (ΔN_{OT}) is studied for NBT stress under a wide range of stress conditions, on p-MOSFETs fabricated using a wide range of gate insulator processing (EOT, nitrogen dose, type of nitridation) condition. ΔN_{OT} is caused by the generation of hot holes under large-stress bias (V_G as well as V_B), which results in high degradation rate and affects V_T shift (ΔV_T) at longer stress time, corrupts extrapolation to end-of-life and, therefore, must be avoided by proper choice of bias during accelerated stress test. With proper NBT stress (absence of hot holes), ΔV_T is due to ΔN_{IT} for a wide range of gate-insulator process (thin and thick PNO and thin TNO, moderate nitrogen dose) and is influenced by INV layer holes and oxide field (E_{OX}). When measured using no-delay technique to nullify recovery-induced artifacts, the time and T dependence of ΔN_{IT} can be explained using the RD model with nondispersive diffusion of molecular hydrogen. The density of nitrogen near the Si–SiO₂ interface (not total dose) influences the magnitude and E_{OX} dependence of ΔN_{IT} , hence ΔV_T . Thicker TNO films with larger interfacial nitrogen density shows ΔN_h (in addition to ΔN_{IT}), which increases the magnitude, but reduces the n and E_A of overall measured ΔV_T .

ACKNOWLEDGMENT

The authors would like to thank D. Varghese, P. Bharath Kumar, G. Gupta, D. Saha, and L. Leela Madhav of IIT Bombay for performing the measurements used in this paper; A. E. Islam and H. Kufrouglu at Purdue University for modeling support; Agere Systems, Renesas Technologies, and Applied Materials for devices and support; and C. Olsen and K. Ahmed (Applied Materials), H. Aono and E. Murakami (Renesas Technologies), A. Krishnan (Texas Instruments), and J. Vasi (IIT Bombay) for useful discussions.

REFERENCES

- [1] B. E. Deal, M. Sklar, A. S. Grove, and E. H. Snow, "Characteristics of the surface-state charge (Q_{ss}) of thermally oxidized silicon," *J. Electrochem. Soc.*, vol. 114, no. 3, pp. 266–273, Mar. 1967.
- [2] K. Uwasawa, T. Yamamoto, and T. Mogami, "A new degradation mode of scaled p⁺ polysilicon gate p-MOSFETs induced by bias temperature (BT) instability," in *IEDM Tech. Dig.*, 1995, pp. 871–874.
- [3] N. Kimizuka, T. Yamamoto, T. Mogami, K. Yamaguchi, K. Imai, and T. Horiuchi, "The impact of bias temperature instability for direct-tunneling ultra-thin gate oxide on MOSFET scaling," in *VLSI Symp. Tech. Dig.*, 1999, pp. 73–74.
- [4] T. Yamamoto, K. Uwasawa, and T. Mogami, "Bias temperature instability in scaled p⁺ polysilicon gate p-MOSFETs," *IEEE Trans. Electron Devices*, vol. 46, no. 5, pp. 921–926, May 1999.
- [5] M. Makabe, T. Kubota, and T. Kitano, "Bias-temperature degradation of p-MOSFETs: Mechanism and suppression," in *Proc. Int. Reliab. Phys. Symp.*, 2000, pp. 205–209.
- [6] G. La Rosa *et al.*, "NBTI-channel hot carrier effects in p-MOSFETs in advanced CMOS technologies," in *Proc. Int. Reliab. Phys. Symp.*, 1997, pp. 282–286.
- [7] P. Chaparala, J. Shibley, and P. Lim, "Threshold voltage drift in p-MOSFETs due to NBTI and HCl," in *Proc. Int. Reliab. Workshop*, 2000, pp. 95–97.
- [8] S. Mahapatra, P. Bharath Kumar, and M. A. Alam, "Investigation and modeling of interface and bulk trap generation during negative bias temperature instability of p-MOSFETs," *IEEE Trans. Electron Devices*, vol. 51, no. 9, pp. 1371–1379, Sep. 2004.
- [9] S. Mahapatra, M. A. Alam, P. Bharath Kumar, T. R. Dalei, and D. Saha, "Mechanism of negative bias temperature instability in CMOS devices: Degradation, recovery and impact of nitrogen," in *IEDM Tech. Dig.*, 2004, pp. 105–108.
- [10] Y. Mitani, M. Nagamine, H. Satake, and A. Toriumi, "NBTI mechanism in ultra-thin gate dielectric—Nitrogen-originated mechanism in SiON," in *IEDM Tech. Dig.*, 2002, pp. 509–512.
- [11] S. S. Tan, T. P. Chen, J. M. Soon, K. P. Loh, C. H. Ang, W. Y. Teo, and L. Chan, "Neighboring effect in nitrogen-enhanced negative bias temperature instability," in *Proc. Solid State Devices and Mater.*, 2003, pp. 70–71.
- [12] S. Tsujikawa, T. Mine, K. Watanabe, Y. Shimamoto, R. Tsuchiya, K. Ohnishi, T. Onai, J. Yugami, and S. Kimura, "Negative bias temperature instability of pMOSFETs with ultra-thin SiON gate dielectrics," in *Proc. Int. Reliab. Phys. Symp.*, 2003, pp. 183–188.
- [13] Y. Mitani, "Influence of nitrogen in ultra-thin SiON on negative bias temperature instability under AC stress," in *IEDM Tech. Dig.*, 2004, pp. 117–120.
- [14] A. T. Krishnan, C. Chancellor, S. Chakravarthi, P. E. Nicollian, V. Reddy, A. Varghese, R. B. Khamankar, and S. Krishnan, "Material dependence of hydrogen diffusion: Implications for NBTI degradation," in *IEDM Tech. Dig.*, 2005, pp. 688–691.
- [15] D. Varghese, D. Saha, S. Mahapatra, K. Ahmed, F. Nouri, and M. Alam, "On the dispersive versus Arrhenius temperature activation of NBTI time evolution in plasma nitrided gate oxides: Measurements, theory, and implications," in *IEDM Tech. Dig.*, 2005, pp. 684–687.
- [16] K. Sakuma, D. Matsushita, K. Muraoka, and Y. Mitani, "Investigation of nitrogen-originated NBTI mechanism in SiON with high-nitrogen concentration," in *Proc. Int. Reliab. Phys. Symp.*, 2006, pp. 454–460.
- [17] G. Gupta, S. Mahapatra, L. Leela Madhav, D. Varghese, K. Ahmed, and F. Nouri, "Interface-trap driven NBTI for ultrathin (EOT \sim 12 Å) plasma and thermal nitrided oxynitrides," in *Proc. Int. Reliab. Phys. Symp.*, 2006, pp. 731–732.

- [18] A. E. Islam, G. Gupta, S. Mahapatra, A. Krishnan, K. Ahmed, F. Nouri, A. Oates, and M. A. Alam, "Gate leakage vs. NBTI in plasma nitrided oxides: Characterization, physical principles, and optimization," in *IEDM Tech. Dig.*, 2006, pp. 329–332.
- [19] S. Mahapatra, K. Ahmed, D. Varghese, A. E. Islam, G. Gupta, L. Madhav, D. Saha, and M. A. Alam, "On the physical mechanism of NBTI in silicon oxynitride p-MOSFETs: Can differences in insulator processing conditions resolve the interface trap generation versus hole trapping controversy?" in *Proc. Int. Reliab. Phys. Symp.*, 2007, pp. 1–9.
- [20] D. Varghese, G. Gupta, L. Madhav, D. Saha, K. Ahmed, F. Nouri, and S. Mahapatra, "Physical mechanism and gate insulator material dependence of generation and recovery of negative-bias temperature instability in p-MOSFETs," *IEEE Trans. Electron Devices*, vol. 54, no. 7, pp. 1672–1680, Jul. 2007.
- [21] E. N. Kumar, V. D. Maheta, S. Purawat, A. E. Islam, C. Olsen, K. Ahmed, M. Alam, and S. Mahapatra, "Material dependence of NBTI physical mechanism in silicon oxynitride (SiON) p-MOSFETs: A comprehensive study by ultra-fast on-the-fly (UF-OTF) I_{DLIN} technique," in *IEDM Tech. Dig.*, 2007, pp. 809–812.
- [22] V. Huard, F. Monsieur, G. Ribes, and S. Bruyere, "Evidence for hydrogen-related defects during NBTI stress in p-MOSFETs," in *Proc. Int. Reliab. Phys. Symp.*, 2003, pp. 178–182.
- [23] V. Huard and M. Denais, "Hole trapping effect on methodology for DC and AC negative bias temperature instability measurements in PMOS transistors," in *Proc. Int. Reliab. Phys. Symp.*, 2004, pp. 40–45.
- [24] M. Denais, C. Parthasarathy, G. Ribes, Y. Rey-Tauriac, N. Revil, A. Bravaix, V. Huard, and F. Perrier, "On-the-fly characterization of NBTI in ultra-thin gate oxide PMOSFETs," in *IEDM Tech. Dig.*, 2004, pp. 109–112.
- [25] T. L. Yang, M. F. Li, C. Shen, C. H. Ang, Z. Chunxiang, Y. C. Yeo, G. Samudra, S. C. Rustagi, and M. B. Yu, "Fast and slow dynamic NBTI components in p-MOSFET with SiON dielectric and their impact on device life-time and circuit application," in *VLSI Symp. Tech. Dig.*, 2005, pp. 92–93.
- [26] H. Reisinger, O. Blank, W. Heinrigs, A. Muhlhoff, W. Gustin, and C. Schlunder, "Analysis of NBTI degradation- and recovery-behavior based on ultra fast V_T measurements," in *Proc. Int. Reliab. Phys. Symp.*, 2006, pp. 448–453.
- [27] C. Shen, M. F. Li, C. E. Foo, T. Yang, D. M. Huang, A. Yap, G. S. Samudra, and Y. C. Yeo, "Characterization and physical origin of fast V_{th} transient in NBTI of pMOSFETs with SiON dielectric," in *IEDM Tech. Dig.*, 2006, pp. 1–4. s.12-p5.
- [28] S. Mahapatra and M. A. Alam, "A predictive reliability model for PMOS bias temperature degradation," in *IEDM Tech. Dig.*, 2002, pp. 505–508.
- [29] P. Bharath Kumar, T. R. Dalei, D. Varghese, D. Saha, S. Mahapatra, and M. A. Alam, "Impact of substrate bias on p-MOSFET negative bias temperature instability," in *Proc. Int. Reliab. Phys. Symp.*, 2005, pp. 700–701.
- [30] C. L. Chen, Y. M. Lin, C. J. Wang, and K. Wu, "A new finding on NBTI lifetime model and an investigation on NBTI degradation characteristic for 1.2 nm ultra thin oxide," in *Proc. Int. Reliab. Phys. Symp.*, 2005, pp. 704–705.
- [31] D. Varghese, S. Mahapatra, and M. A. Alam, "Hole energy dependent interface trap generation in MOSFET Si/SiO₂ interface," *IEEE Electron Device Lett.*, vol. 26, no. 8, pp. 572–574, Aug. 2005.
- [32] S. Mahapatra, D. Saha, D. Varghese, and P. Bharath Kumar, "On the generation and recovery of interface traps in MOSFETs subjected to NBTI, FN and HCI stress," *IEEE Trans. Electron Devices*, vol. 53, no. 7, pp. 1583–1592, Jul. 2006.
- [33] S. Rangan, N. Mielke, and E. C. C. Yeh, "Universal recovery behavior of negative bias temperature instability," in *IEDM Tech. Dig.*, 2003, pp. 341–344.
- [34] M. Ershov, S. Saxena, H. Karbasi, S. Winters, S. Minehane, J. Babcock, R. Lindley, P. Clifton, M. Redford, and A. Shibkov, "Dynamic recovery of negative bias temperature instability in p-type metal-oxide-semiconductor field-effect transistors," *Appl. Phys. Lett.*, vol. 83, no. 8, pp. 1647–1649, Aug. 2003.
- [35] A. E. Islam, H. Kufuoglu, D. Varghese, S. Mahapatra, and M. A. Alam, "Recent issues in negative-bias temperature instability: Initial degradation, field dependence of interface trap generation, hole trapping effects and relaxation," *IEEE Trans. Electron Devices*, vol. 54, no. 9, pp. 2143–2154, Sep. 2007.
- [36] A. E. Islam, E. N. Kumar, H. Das, S. Purawat, V. Maheta, H. Aono, E. Murakami, S. Mahapatra, and M. A. Alam, "Theory and practice of ultra-fast measurements for NBTI degradation: Challenges and opportunities," in *IEDM Tech. Dig.*, 2007, pp. 813–816.
- [37] K. O. Jeppson and C. M. Svensson, "Negative bias stress of MOS devices at high electric fields and degradation of MNOS devices," *J. Appl. Phys.*, vol. 48, no. 5, pp. 2004–2014, May 1977.
- [38] S. Ogawa and N. Shiono, "Generalized diffusion-reaction model for the low-field charge-buildup instability at the Si-SiO₂ interface," *Phys. Rev. B, Condens. Matter*, vol. 51, no. 7, pp. 4218–4230, Feb. 1995.
- [39] G. V. Gadiyak, "Numerical simulation of hydrogen redistribution in thin SiO₂ films under electron injection in high fields," *Appl. Surf. Sci.*, vol. 113/114, pp. 627–630, Apr. 1997.
- [40] A. Haggag, W. McMahan, K. Hess, K. Cheng, J. Lee, and J. Lyding, "High-performance chip reliability from short-time-tests-statistical models for optical interconnect and HCI/TDDDB/NBTI deep-submicron transistor failures," in *Proc. Int. Reliab. Phys. Symp.*, 2001, pp. 271–279.
- [41] M. Alam, "A critical examination of the mechanics of dynamic NBTI for p-MOSFETs," in *IEDM Tech. Dig.*, 2003, pp. 345–348.
- [42] S. Chakravarthi, A. T. Krishnan, V. Reddy, C. F. Machala, and S. Krishnan, "A comprehensive framework for predictive modeling of negative bias temperature instability," in *Proc. Int. Reliab. Phys. Symp.*, 2004, pp. 273–282.
- [43] M. Alam and S. Mahapatra, "A comprehensive model of PMOS NBTI degradation," *Microelectron. Reliab.*, vol. 45, no. 1, pp. 71–81, Jan. 2005.
- [44] S. Zafar, "Statistical mechanics based model for negative bias temperature instability induced degradation," *J. Appl. Phys.*, vol. 97, no. 10, pp. 103 709-1–103 709-9, May 2005.
- [45] B. Kaczer, V. Arkhipov, R. Degraeve, N. Collaert, G. Groeseneken, and M. Goodwin, "Disorder-controlled-kinetics model for negative bias temperature instability and its experimental verification," in *Proc. Int. Reliab. Phys. Symp.*, 2005, pp. 381–387.
- [46] T. Grasser, W. Gos, V. Sverdlov, and B. Kaczer, "The universality of NBTI relaxation and its implications for modeling and characterization," in *Proc. Int. Reliab. Phys. Symp.*, 2007, pp. 268–280.
- [47] J. De Blauwe, J. Van Houdt, D. Wellekens, G. Groeseneken, and H. E. Maes, "SILC related effects in flash E²PROMs—Part I: A quantitative model for steady state SILC," *IEEE Trans. Electron Devices*, vol. 45, no. 8, pp. 1745–1750, Aug. 1998.
- [48] M. Alam, "SILC as a measure of trap generation and predictor of T_{BD} in ultrathin oxides," *IEEE Trans. Electron Devices*, vol. 49, no. 2, pp. 226–231, Feb. 2002.
- [49] D. J. DiMaria and E. Cartier, "Mechanism for stress-induced leakage currents in thin silicon dioxide films," *J. Appl. Phys.*, vol. 78, no. 6, pp. 3883–3894, Sep. 1995.
- [50] M. Alam, J. Bude and A. Ghetti, "Field acceleration for oxide breakdown—Can an accurate anode hole injection model resolve the E vs. 1/E controversy?" in *Proc. Int. Reliab. Phys. Symp.*, 2000, pp. 21–26.
- [51] J. D. Bude, B. E. Weir, and P. Silverman, "Explanation of stress-induced damage in thin oxides," in *IEDM Tech. Dig.*, 1998, pp. 179–182.
- [52] S. Takagi, N. Yasuda, and M. Toriumi, "Experimental evidence of inelastic tunneling in stress-induced leakage current," *IEEE Trans. Electron Devices*, vol. 46, no. 2, pp. 335–341, Feb. 1999.
- [53] G. Groeseneken and H. E. Maes, "Basics and applications of charge pumping in submicron MOSFETs," *Microelectron. Reliab.*, vol. 38, no. 9, pp. 1379–1389, Sep. 1998.
- [54] P. A. Kraus, K. Z. Ahmed, C. S. Olsen, and F. Nouri, "Physical models for predicting plasma nitrided Si-O-N gate dielectric properties from physical metrology," *IEEE Electron Device Lett.*, vol. 24, no. 9, pp. 559–561, Sep. 2003.
- [55] J. R. Shallenberger, D. A. Cole, and S. W. Novak, "Characterization of silicon oxynitride thin films by x-ray photoelectron spectroscopy," *J. Vac. Sci. Technol. A, Vac. Surf. Films*, vol. 17, no. 4, pp. 1086–1090, Jul. 1999.
- [56] S. Rauf, S. Lim, and P. L. G. Ventzek, "Model for nitridation of nanoscale SiO₂ thin films in pulsed inductively coupled N₂ plasma," *J. Appl. Phys.*, vol. 98, no. 2, pp. 024 305.1–024 305.10, Jul. 2005.
- [57] V. Reddy, A. T. Krishnan, A. Marshall, J. Rodriguez, S. Natarajan, T. Rost, and S. Krishnan, "Impact of negative bias temperature instability on digital circuit reliability," in *Proc. Int. Reliab. Phys. Symp.*, 2002, pp. 248–254.
- [58] J. H. Stathis, G. LaRosa, and A. Chou, "Broad energy distribution of NBTI-induced interface states in p-MOSFETs with ultra-thin nitrided oxide," in *Proc. Int. Reliab. Phys. Symp.*, 2004, pp. 1–7.
- [59] M. A. Alam, "A simple view of a complex phenomenon," in *Proc. Int. Reliab. Phys. Symp.*, 2006. NBTI tutorial.
- [60] M. L. Reed and J. D. Plummer, "Chemistry of Si-SiO₂ interface trap annealing," *J. Appl. Phys.*, vol. 63, no. 12, pp. 5776–5793, Jun. 1988.



Souvik Mahapatra (S'99–M'99–SM'07) received the Ph.D. degree in electrical engineering from the Indian Institute of Technology (IIT), Bombay, Mumbai, India, in 1999.

From 2000 to 2001, he was with Bell Laboratories, Murray Hill, NJ. Since 2002, he has been with the Department of Electrical Engineering, IIT, Bombay, where he is currently an Associate Professor. He has published more than 70 papers in referred international journals and conference proceedings. His research interests include CMOS device and flash

memory reliability.

Dr. Mahapatra delivered invited talks at major international conferences, including the IEEE International Electron Devices Meeting, given tutorials at the IEEE International Reliability Physics Symposium, and served as a Reviewer for several international journals and conference proceedings.



Muhammad Ashraf Alam (M'96–SM'01–F'06) received the B.S.E.E. degree from Bangladesh University of Engineering and Technology, Dhaka, Bangladesh, in 1988, the M.S. degree from Clarkson University, Potsdam, NY, in 1991, and the Ph.D. degree from Purdue University, West Lafayette, IN, in 1994, all in electrical engineering.

From 1995 to 2001, he was with the Silicon ULSI Research Department, Bell Laboratories, Lucent Technologies, Murray Hill, NJ, as a member of Technical Staff. From 2001 to 2003, he was with

Agere Systems, Murray Hill, NJ, as a Distinguished Member of Technical Staff. Since 2004, he has been with the School of Electrical Engineering and Computer Science, Purdue University, as a Professor of electrical and computer engineering. He has published more than 80 papers in international journals. His research and teaching focus on physics, simulation, characterization, and technology of classical and emerging electronic devices, including the theory of oxide reliability, nanocomposite thin film transistors, and nanobio sensors.

Dr. Alam is a member of Sigma Xi. He is a recipient of the 2006 IEEE Kiyo Tomiyasu Award for his contributions to device technology for communication systems. He has presented many invited and contributed talks at international conferences.